Spin-orbital ordering and mesoscopic phase separation in the double perovskite Ca_2FeReO_6

E. Granado,[1,2,*] Q. Huang,[1,3] J. W. Lynn,[1,2] J. Gopalakrishnan,[2,4] R. L. Greene,[2] and K. Ramesha[4]
[1]*NIST Center for Neutron Research, National Institute of Standards and Technology, Gaithersburg, Maryland 20899*
[2]*Center for Superconductivity Research, University of Maryland, College Park, Maryland 20742*
[3]*Materials Engineering Program, University of Maryland, College Park, Maryland 20742*
[4]*Solid State and Structural Chemistry Unit, Indian Institute of Science, Bangalore 560012, India*
(Received 1 April 2002; revised manuscript received 7 May 2002; published 6 August 2002)

Neutron powder diffraction measurements on Ca_2FeReO_6 reveal that this double perovskite orders ferrimagnetically and shows anomalous lattice parameter behavior below $T_C = 521$ K. Below ~ 300 K and ~ 160 K we observe that the high-T monoclinic crystal structure separates into two and three monoclinic phases, respectively. A magnetic field suppresses the additional phases at low T in favor of the highest-T phase. These manifestations of the orbital degree of freedom of Re $5d$ electrons indicate that these electrons are strongly correlated and the title compound is a Mott insulator, with competing spin-orbitally ordered states.

DOI: 10.1103/PhysRevB.66.064409 PACS number(s): 75.30.Gw, 61.12.Ld, 64.75.+g, 75.25.+z

I. INTRODUCTION

Novel phenomena caused by electrons localized in degenerate orbital states have been the central issue in the physics of transition-metal oxides for the last few years. For e_g orbital systems, the degeneracy under cubic crystalline fields is often removed by large Jahn-Teller distortions of the oxygen octahedra. The physics of electrons localized in partly occupied t_{2g} orbitals is quite different, due to the relative weakness of the Jahn-Teller coupling, higher degeneracy, and additional symmetry of t_{2g} orbitals. In addition, these electrons may show unquenched orbital magnetic moments, and spin-orbit coupling usually plays an important role.

The double-perovskite compounds $A_2Fe(Mo,Re)O_6$ (A = Ca, Sr, or Ba) have recently attracted much scientific and technological interest after the discovery of large tunneling magnetoresistance at room temperature in most cases,[1–6] which has been ascribed to half-metallic electronic band structures.[1,2,7–11] An intriguing exception is the insulating behavior found in the compound Ca_2FeReO_6 (CFRO),[3] revealing that the (Fe,Re)-based double perovskites are at the border of a metal-insulator transition.[4] Mössbauer studies in CFRO indicate the presence of Fe^{3+} ions;[4] thus the oxidation state of Re ions is expected to be $5+$, with two electrons in the $5d$ t_{2g} orbitals. In order to search for possible manifestations of the Re t_{2g} orbital degree of freedom[12] in this insulating compound, the nuclear and magnetic structures were investigated by neutron powder diffraction. A number of remarkable observations were made, to be described in this paper: (i) mesoscopic phase separations, with coexisting monoclinic crystal structures below ~ 300 K and large changes in the phase proportions below $T_s \sim 160$ K; (ii) magnetic-field (H) control of the volume fractions in the phase-separated state at 100 K, with a suppression of the additional phases observed below ~ 300 K for an applied field of a few tesla; (iii) a ferrimagnetic arrangement of Fe and Re magnetic moments below $T_C = 521$ K, with strong evidence for distinct moment directions for the competing phases; (iv) anomalous lattice parameter behavior below T_C; and (v) a new Bragg peak below T_s, which is forbidden by the symmetry considered to model the nuclear structure. These results indicate that the Re^{5+} t_{2g}^2 electrons are localized on an atomic scale and CFRO is a Mott insulator. The mesoscopic phase separations observed for this compound are ascribed to a competition between distinct spin and orbitally ordered insulating states.

II. EXPERIMENTAL DETAILS

The preparation procedures and characterization of the ceramic pellets of CFRO used in this work are described in Refs. 3 and 4. The high-resolution neutron powder diffraction measurements were performed on the BT-1 powder diffractometer at NIST Center for Neutron Research, using monochromatic beams with $\lambda = 1.5402(1)$ Å, 1.5903(1) Å, and 2.0783(1) Å, produced by Cu(311), Si(531), and Ge(311) monochromators, respectively. Typical collimations were 15′, 20′, and 7′ arc before and after the monochromator, and before detectors, respectively. The intensities were measured in steps of 0.05° in the 2θ range 3°–168°. Data were collected at various temperatures in the range 10–650 K. Crystal and magnetic structure refinements were carried out using the program GSAS.[13] The nuclear scattering amplitudes are 0.490, 0.954, 0.920, and 0.581 ($\times 10^{-14}$ m) for Ca, Fe, Re, and O, respectively.[13] T-dependent measurements were performed on warming the sample.

III. RESULTS AND ANALYSIS

Above ~ 520 K, we found that this compound is nonmagnetic and exhibits monoclinic structure with $P2_1/n$ symmetry and the unit cell size $\approx \sqrt{2}a_p \times \sqrt{2}a_p \times 2a_p$ and $\beta \approx 90°$,[14] where a_p is the unit-cell size of the primitive perovskite. Initial structural parameters used in the refinement were taken from Ref. 4. A minor Fe_3O_4 impurity (0.6% weight fraction) was identified. Due to the small phase fraction of this impurity phase, a simplified cubic spinel unit cell (space group $Fd3m$) was used in the refinements at all T, despite the well-known Verwey transition to a monoclinic superstructure below ~ 120 K.[15–19] Concerning the main phase, the refined occupancies are 0.93(2), 0.96(2), 1, and 0.98(2)

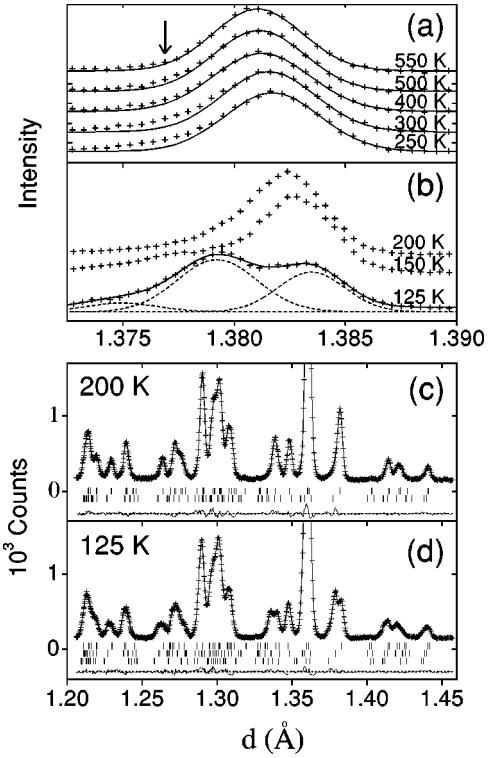

FIG. 1. (a),(b) Crosses: *T*-dependence of the neutron powder diffraction of Ca_2FeReO_6 around the (040) Bragg reflection, at $250K \leqslant T \leqslant 550$ K (a) and $125\,\mathrm{K} \leqslant T \leqslant 200$ K (b). The solid lines in (a) are Gaussian curves. The lines in (b) illustrate a three-Gaussian fit for the scattering at $T = 125$ K. (c),(d) Crosses: selected portion of the neutron powder profile of Ca_2FeReO_6 at $T = 200$ K (c) and $T = 125$ K (d). The solid lines indicate the calculated profiles using two (c) and three (d) distinct monoclinic phases as the structural model (see text). The differences between experimental and calculated profiles are given as solid lines in the bottom of the figures. Short vertical lines correspond to Bragg peak positions for M1 and M2 (c) and M1, M2, and SP (d).

for Ca, Fe, Re, and O, respectively. Quoted errors in this manuscript are statistical and represent one standard deviation. Due to the similar neutron scattering lengths of Fe and Re, the degree of Fe and Re ionic ordering in our sample was not estimated by neutron diffraction. Previous x-ray diffraction studies[2,4] indicated that the Fe/Re double-perovskite system has a strong tendency for ionic ordering ($\sim$95% for our sample[4]).

Phase separations were observed for CFRO. Figure 1(a) shows the (040) nuclear reflection for $250\,\mathrm{K} \leqslant T \leqslant 550$ K. Gaussian solid lines fitting the higher-*d*-spacing side of the peak are also displayed. At 550 K, the good fit indicates a single peak, within our resolution. Below $\sim$500 K, however, a residual intensity which increases with decreasing *T* is observed on the lower-*d*-spacing side, suggesting the presence of a second peak. Below $\sim$300 K, we were able to obtain stable refinements including a second monoclinic phase in the model, which improved significantly the overall fit to the observed intensities. This phase is referred to as M2.[20] As shown in Fig. 1(b), the intensity on the lower-*d*-spacing side of the (040) reflection increases sharply, and this reflection

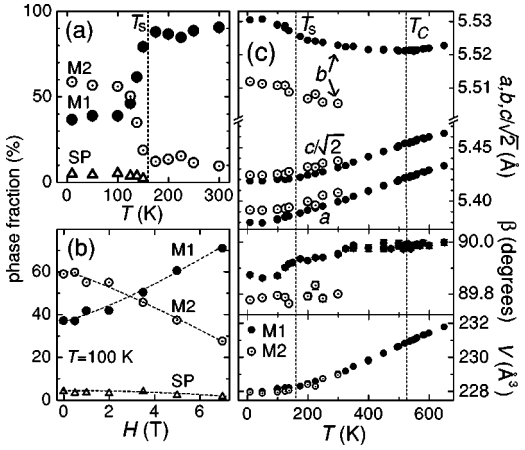

FIG. 2. (a) *T* dependence of the relative fractions of coexisting phases M1, M2, and SP for Ca_2FeReO_6. (b) Magnetic-field dependence of the relative fractions of M1, M2, and SP at 100 K. The dashed lines are guides to the eyes. (c) *T* dependence of the lattice parameters *a*, *b*, and *c*, monoclinic angle β, and unit cell volume *V* of M1 (solid circles), and M2 (open circles). Error bars are smaller than the symbol sizes.

becomes three peaks below $T_s \sim 160$ K. A three-Gaussian fit at 125 K is illustrated (lines). In the final refinements below T_s, excellent fits were obtained by using three monoclinic phases (M1, M2, and SP), with slightly different lattice parameters. At 540 K, in the single-phase regime (besides the Fe_3O_4 impurity phase), the coefficients describing the Bragg peak linewidths indicate a lattice strain of 0.22(1)% full width at half maximum (FWHM) for CFRO. Below 300 K, where phase separations were clearly observed, such coefficients had to be constrained to be the same for the coexisting CFRO phases, in order to avoid large correlations between the fitting parameters. Under this constraint, an average lattice strain of 0.35(2)% FWHM was inferred for the coexisting CFRO phases at 100 K, larger than the strain for the single CFRO phase at 540 K. No particle size broadening was observed at 100 K, within our resolution, indicating that the M1 and M2 domains are larger than $\sim$1000 Å. Figures 1(c) and 1(d) show a portion of the observed and calculated intensities for models with two phases (200 K) and three phases (125 K), respectively.

Figure 2(a) shows the M1, M2, and SP phase fractions in the *T* interval in which multiphase Rietveld refinements were performed ($\leqslant$300 K). Above 300 K, a small fraction of M2 ($\leqslant$5%) may be still present [see Fig. 1(a)]. The M2 fraction remains nearly constant at $\sim$12% between $\sim$300 K and T_s, rapidly develops to $\sim$55% below T_s, and then remains constant again below $\sim$100 K. The SP fraction develops up to $\sim$5% below T_s.

Figure 2(b) shows the *H* dependence of the M1, M2, and SP fractions. The magnetic field was applied using a superconducting vertical-field magnet after zero-field (ZF) cooling the sample to 78 K, followed by a ZF warming to 100 K. The profiles were analyzed under the same structural model described above. Only high-angle data with negligible magnetic contributions were used in the refinement of the nuclear structure under applied *H*. The magnetic field suppresses the

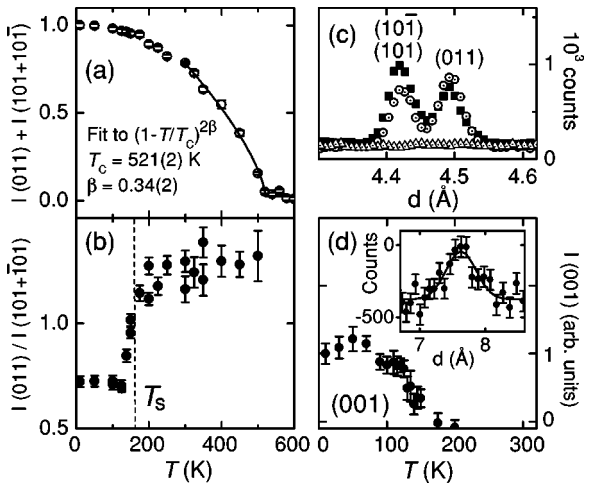

FIG. 3. (a) T dependence of the sum of intensities of the (011), (101), and $(10\bar{1})$ Bragg peaks for Ca_2FeReO_6, normalized at 10 K. The solid line is a fit to a power law, giving $T_C = 521(2)$ K, and a critical exponent $\beta = 0.34(2)$. (b) T dependence of the ratio of the intensity of the (011) reflection and the sum of the (101) and $(10\bar{1})$ (unresolved) Bragg reflections. (c) The data at $T = 100$ K (solid squares), $T = 200$ K (open circles), and $T = 550$ K (open triangles). (d) T dependence of the intensity of the peak at the (001) position. The inset shows the data at 10 K, subtracted from 300 K, and a Gaussian fit.

M2 fraction, from 55% to 22%, as the field increases to 7 T. The original phase fractions are fully restored after the release of H.

Magnetic intensities superposed on the nuclear Bragg peaks were observed at low angles below ~ 520 K. Figure 3(a) shows the sum of the integrated intensities of the (011), (101), and $(10\bar{1})$ reflections as a function of T, indicating that the magnetic ordering occurs below 521 K (T_C), in reasonable agreement with $T_C \sim 540$ K obtained by magnetization measurements.[21,22] Above T_s, a ferrimagnetic model for the Fe and Re moments (M_{Fe} and M_{Re}, respectively) lying in the ac plane gives a good fit to the observed data. The angle between the moments and the a axis is $\varphi = 55(2)°$, obtained at 400 K, and remains constant within two standard errors for $T_s < T < T_C$. As shown in Fig. 3(b), the ratio of the (011) and $(101)+(10\bar{1})$ intensities remains constant above T_s, agreeing with the conclusion that the spin direction does not change in this T range. Below T_s, this ratio decreased sharply [see also Fig. 3(c)], indicating a change in the average spin structure, and then remained constant below ~ 100 K. This behavior is clearly related to the phase separation. The constant moment direction ($\hat{\mathbf{m}}$) above T_s allows us to assume that $\hat{\mathbf{m}}(\mathrm{M1})$ does not change with T. We then modeled the magnetic structure below T_s, keeping $\hat{\mathbf{m}}(\mathrm{M1})$ fixed and allowing $\hat{\mathbf{m}}(\mathrm{M2}) \neq \hat{\mathbf{m}}(\mathrm{M1})$, and found that $\hat{\mathbf{m}}(\mathrm{M2})$ is nearly parallel ($\pm 5°$) to the b axis. The sharp changes in the relative intensities of the magnetic peaks between 100 K and T_s are due to the changes of the M1 and M2 phase proportions [see Fig. 2(a)]. The moments were constrained to be the same for M1, M2, and SP in the final refinements, yielding $M_{Fe} = 3.42(7)\mu_B$ and $M_{Re} = 1.02(7)\mu_B$ at 10 K, pointing in opposite directions. These values agree reasonably well with $(3.76–4.29)\mu_B$ and $(1.07–1.33)\mu_B$ for Fe and Re, respectively, predicted by band structure calculations for this compound.[9]

The T dependence of the lattice parameters for M1 and M2 is shown in Fig. 2(c). For M1, the a and c axes decrease smoothly as T decreases, while the b axis shows a negative thermal expansion for $T \lesssim 520\,\mathrm{K} \approx T_C$, crossing over to conventional behavior above T_C. This effect was not observed in the metallic isostructural compound Ca_2FeMoO_6.[23,24] According to our refinements, the monoclinic angle $\beta(M1)$ is very close to 90° above ~ 300 K and shows inflection points at ~ 300 K and T_s. This result suggests that the crystal structure of M1 is distorted by the phase separation. The unit-cell volume decreases smoothly for decreasing T and does not indicate any metal-insulator transition for this compound. Compared to M1, M2 has shorter b, longer a and c, smaller β, and slightly smaller V. The application of a magnetic field $H \leqslant 7$ T at 100 K is responsible for a slight ($\lesssim 0.01$ Å) decrease of the b axes, increase of the a and c axes, and no significant changes in β and V for both M1 and M2.

The average bond distances between the transition metal (M) and oxygen ions in the MO_6 octahedra are 2.02 Å and 1.95 Å at room temperature for the two independent crystallographic M sites in the $P2_1/n$ symmetry. Based on considerations of the ionic radius, the bond distance of 2.02 Å would favor either Fe^{3+} or Re^{4+} ions, and that of 1.95 Å would favor either Re^{5+} or Fe^{4+}; because the neutron scattering lengths of Fe and Re are similar, we cannot identify the M sites directly from the refinement. Since a Mössbauer spectrum on this sample[4] is consistent with Fe^{3+}, we conclude that the largest M ion corresponds to Fe^{3+}, while the smallest M ion is Re^{5+}. The differences of Fe-O distances are very small [from 2.010(4) Å to 2.033(3) Å], as well as of Re-O distances [from 1.945(4) Å to 1.954(3) Å]. Also, the O-M-O angles are very close to 90° ($\pm 1°$), indicating a very small distortion for the MO_6 octahedra. Bond-valence calculations[25] using the refined Fe-O distances give a valence of $+2.94$ for Fe. The changes in the M-O bond distances with T and between M1 and M2 are very small, within three standard errors, showing that M1 and M2 cannot be easily discerned on the basis of the Fe and Re oxidation states. No anomalous changes in the bond distances caused by the phase separation could be observed in our experiment.

In order to search for weak Bragg reflections, complementary measurements were taken on the BT-2 triple-axis spectrometer at NIST with $\lambda = 2.359$ Å and relaxed collimations, providing much stronger signal than the high-resolution measurements. The inset of Fig. 3(d) shows the energy-integrated neutron scattering at high d spacings, at 10 K subtracted from 300 K. We observed a weak peak at $d = 7.62(3)$ Å close to the (001) position for CFRO. The integrated intensity is as weak as $\sim 0.1\%$ of the strongest nuclear Bragg peak, 1.2(2)% of the sum of the $(011)+(101)+(10\bar{1})$ magnetic intensities at 10 K, and $\sim 5\%$ of the principal Bragg peaks of the Fe_3O_4 impurity phase. An attempt to determine the nuclear or magnetic nature of this peak di-

rectly by polarization analysis was unsuccessful, since the neutron beam was depolarized by the sample. This peak likely originates from M2, given the clear correlation of its intensity with the M2 phase fraction [see Figs. 2(a) and 3(d)]. On the other hand, the crystal structure of the Fe_3O_4 impurity phase is distorted from cubic symmetry with cell parameter a^* to a monoclinic $\sqrt{2}a^* \times \sqrt{2}a^* \times 2a^*$ supercell with Cc space group symmetry below ~ 120 K.[15–19] Thus, (1,0,1/2) and (0,1,1/2) superstructure Bragg peaks (cubic notation) from Fe_3O_4 might be expected below 120 K, at $d = 7.504(3)$ Å using the refined a^* for our impurity phase or at $d = 7.514\,44(3)$ Å and $d = 7.496\,97(3)$ Å using the extended monoclinic cell and lattice parameters reported in Ref. 19. However, the differences between the d spacing for the forbidden Bragg peak observed for CFRO and the expected positions for the superstructure reflections for Fe_3O_4 are statistically significant (about four standard deviations). Second, the intensities of the strongest Fe_3O_4 superlattice peaks are typically $\lesssim 1\%$ of those of the principal peaks.[19] Since Fe_3O_4 superlattice peaks with wave vectors (1,0,1/2) and (0,1,1/2) were found to be particularly weak,[18] these reflections are expected to much weaker than the observed peak at $d = 7.62(3)$ Å and low T for our sample. We also note that significant intensities were observed for this peak between 120 K and 150 K, therefore above the Verwey transition for Fe_3O_4. We conclude that this peak cannot be ascribed to the impurity phase and it is due to CFRO. There are thus two possible origins of this peak: (i) a nuclear reflection related to a symmetry reduction, since this peak is forbidden by $P2_1/n$ symmetry. However, we were not able to model a lower symmetry to refine the structure of either M1 or M2, since the intensities of the peak at (001) position and any other forbidden reflections are too weak to be detected in high-resolution measurements. (ii) An antiferromagnetic canting in the Re and/or Fe magnetic sublattices, with the propagation vector along one particular Fe-Re-Fe binding direction.

In order to search for spin excitations in CFRO at room temperature, inelastic neutron scattering measurements were performed close to the (000) reciprocal lattice point, using the BT-9 triple-axis spectrometer at NIST. Details of the method are given in Ref. 26. The incident energy was chosen to be 13.5 meV, and collimations of 10′-10′-10′-10′ FWHM were used. No excitations were detected within our experimental range. We note that the accessible window in energy-momentum space is very limited around the (000) Bragg point, and the nonobservation of spin excitations is indicative of a gap larger than ~ 0.5 meV in the spin-wave dispertion or, alternatively, a spin stiffness constant larger than ~ 200 meV Å^2 at room temperature.

IV. DISCUSSION

The anomalous expansion of the b-lattice parameter for decreasing T below T_C [see Fig. 2(c)] clearly suggests a simultaneous spin and orbital-ordering transition, which can be ascribed to a significant spin-orbit coupling of t_{2g} electrons with unquenched orbital magnetic moments. We attribute this to the Re^{5+} orbital degree of freedom, since high-spin Fe^{3+} ions are not orbitally active.

Phase separations occur in our CFRO sample below room temperature, indicating a close competition between distinct physical states with similar free energies over a large T interval. The delicate energetic balance between these states is demonstrated by the decisive influence of a magnetic field of the order of a few tesla on the phase fractions at 100 K. Considering such a close competition, it is clear that even a slight degree of chemical disorder and inhomogeneity may stabilize the phase-separated state against a more conventional first-order transition at a definite temperature. Below ~ 160 K (T_s), three coexisting phases were detected (M1, M2, and SP). The SP fraction is small at all T and may be a strain phase which underlies the coexistence of M1 and M2. Concerning the main phases, their fractions being tuned by an applied magnetic field at 100 K shows that M1 and M2 have distinct magnetic structures. A simple collinear ferrimagnetic model was sufficient to obtain a satisfactory refinement of our high-resolution data below T_C, with different moment orientations for M1 and M2 below T_s. On the other hand, high-intensity measurements reveal a weak peak below T_s at the (001) position, which intensity correlates with the M2 fraction, indicating a noncollinear magnetic structure or, alternatively, a symmetry reduction for M2. Both possibilities suggest that M2 represents an orbitally ordered pattern of the Re^{5+} t_{2g} electrons which is distinct from the orbitally ordered structure of M1.

Extensive research has shown that mesoscopic phase separation plays a key role in the colossal magnetoresistance effect observed for a number of manganite compounds, where insulating and metallic coexisting phases may be tuned by applied magnetic fields.[27] Although CFRO is also close to a metal-insulator transition,[4] the resistivity of this compound shows monotonic insulating behavior below room temperature (Ref. 3); therefore, neither M1 nor M2 seems to be metallic. In fact, our results suggest that the orbital degree of freedom, characteristic of a Mott insulating state, is manifested for both phases, implying that the Re $5d$ electrons are strongly correlated. Recent theoretical investigations in $Sr_2Fe(Re,Mo)O_6$ double-perovskite systems support an enhanced effective intra-atomic exchange strength at the Mo or Re site (I_{eff}), due to hybridization with the Fe $3d$ electrons.[7,8] The possibility of a negative effective Coulomb interaction strength $U_{eff} = U - I_{eff}$ due to the enhanced I_{eff} was proposed for Sr_2FeMoO_6.[7] For monoclinic CFRO, the Re t_{2g}–Fe t_{2g} hybridization is reduced due to the significant bending of the Fe-O-Re angle;[9] therefore, smaller values of I_{eff} may be expected. This fact, coupled with the possibly larger U for the Re than for the Mo electrons, may lead to a relatively large U_{eff} for the Re site in CFRO, which may partly account for the Mott insulating state inferred from our experimental data.

ACKNOWLEDGMENTS

We thank A. Santoro, S. Trevino, and D.C. Dender for helpful discussions. This work was supported by NSF-MRSEC, Grant No. DMR 00-80008, U.S., FAPESP, Brazil, and DST, New Delhi, India.

*Present address: Laboratório Nacional de Luz Síncrotron, Caixa Postal 6192, CEP 13083-970, Campinas, SP, Brazil.

[1] K.-I. Kobayashi, T. Kimura, H. Sawada, K. Terakura, and Y. Tokura, Nature (London) **395**, 677 (1998).

[2] K.-I. Kobayashi, T. Kimura, Y. Tomioka, H. Sawada, K. Terakura, and Y. Tokura, Phys. Rev. B **59**, 11 159 (1999).

[3] W. Prellier, V. Smolyaninova, A. Biswas, C. Galley, R.L. Greene, K. Ramesha, and J. Gopalakrishnan, J. Phys. C **12**, 965 (2000).

[4] J. Gopalakrishnan, A. Chattopadhyay, S.B. Ogale, T. Venkatesan, R.L. Greene, A.J. Millis, K. Ramesha, B. Hannoyer, and G. Marest, Phys. Rev. B **62**, 9538 (2000).

[5] A. Maignan, B. Raveau, C. Martin, and M. Hervieu, J. Solid State Chem. **144**, 224 (1999).

[6] J.M. Dai, W.H. Song, S.G. Wang, S.L. Ye, K.Y. Wang, J.J. Du, Y.P. Sun, J. Fang, J.L. Chen, and B.J. Gao, Mater. Sci. Eng., B **83**, 217 (2001).

[7] D.D. Sarma, P. Mahadevan, T. Saha-Dasgupta, S. Ray, and A. Kumar, Phys. Rev. Lett. **85**, 2549 (2000).

[8] Z. Fang, K. Terakura, and J. Kanamori, Phys. Rev. B **63**, 180407(R) (2001).

[9] H. Wu, Phys. Rev. B **64**, 125126 (2001).

[10] A. Chattopadhyay and A.J. Millis, Phys. Rev. B **64**, 024424 (2001).

[11] A.A. Aligia, P. Petrone, J.O. Sofo, and B. Alascio, Phys. Rev. B **64**, 092414 (2001).

[12] Y. Tokura and N. Nagaosa, Science **288**, 462 (2000).

[13] C. Larson and R. B. Von Dreele (unpublished).

[14] For a review of structural aspects of double-perovskite systems, see M.T. Anderson, K.B. Greenwood, G.A. Taylor, and K.R. Poeppelmeier, Prog. Solid State Chem. **22**, 197 (1993).

[15] E.J.W. Verwey, P.W. Haayman, and F.C. Romeijan, J. Chem. Phys. **15**, 181 (1947).

[16] M. Iizumi and G. Shirane, Solid State Commun. **17**, 433 (1975).

[17] J. Yoshido and S. Iida, J. Phys. Soc. Jpn. **47**, 1627 (1979).

[18] M. Iizumi, T.F. Koetzle, G. Shirane, S. Chikazumi, M. Matsui, and S. Todo, Acta Crystallogr., Sect. B: Struct. Crystallogr. Cryst. Chem. **38**, 2121 (1982).

[19] J.P. Wright, J.P. Attfield, and P.G. Radaelli, Phys. Rev. Lett. **87**, 266401 (2001).

[20] For an independent report also showing evidence for phase separation in Ca_2FeReO_6, see W. Westerburg, O. Lang, C. Ritter, C. Felser, W. Tremel, and G. Jakob, Solid State Commun. **122**, 201 (2002).

[21] J. Longo and R. Ward, J. Am. Chem. Soc. **83**, 2816 (1961).

[22] S.E. Lofland, T. Scabarozi, S. Kale, S.M. Bhagat, S.B. Ogale, T. Venkatesan, R.L. Greene, J. Gopalakrishnan, and K. Ramesha, IEEE Trans. Magn. **37**, 2153 (2001).

[23] J.A. Alonso, M.T. Casais, M.J. Martínez-Lope, J.L. Martínez, P. Velasco, A. Muñoz, and M.T. Fernández-Díaz, Chem. Mater. **12**, 161 (2000).

[24] L. Pinsard-Gaudart, R. Surynarayanan, A. Revcolevschi, J. Rodriguez-Carvajal, J-M. Greneche, P.A.I. Smith, R.M. Thomas, R.P. Borges, and J.M.D. Coey, J. Appl. Phys. **87**, 7118 (2000).

[25] I.D. Brown, Acta Crystallogr., Sect. B: Struct. Sci. **48**, 553 (1992).

[26] J.W. Lynn, R.W. Erwin, J.A. Borchers, Q. Huang, A. Santoro, J-L. Peng, and Z.Y. Li, Phys. Rev. Lett. **76**, 4046 (1996).

[27] See E. Dagotto, T. Hotta, and A. Moreo, Phys. Rep. **344**, 1 (2001), and references therein.